

Species interactions reproduce abundance correlation patterns in microbial communities

José Camacho-Mateu,¹ Aniello Lampo,¹ Matteo Sireci,^{2,3} Miguel Ángel Muñoz,^{2,3} and José A. Cuesta^{1,4}

¹*Grupo Interdisciplinar de Sistemas Complejos (GISC),*

Departamento de Matemáticas, Universidad Carlos III de Madrid, Leganés, Spain

²*Departamento de Electromagnetismo y Física de la Materia, Universidad de Granada, Granada, Spain*

³*Instituto Carlos I de Física Teórica y Computacional, Universidad de Granada, Granada, Spain*

⁴*Instituto de Biocomputación y Física de Sistemas Complejos (BIFI), Universidad de Zaragoza, Zaragoza, Spain*

During the last decades macroecology has identified broad-scale patterns of abundances and diversity of microbial communities and put forward some potential explanations for them. However, these advances are not paralleled by a full understanding of the underlying dynamical processes. In particular, abundance fluctuations over metagenomic samples are found to be correlated, but reproducing these through appropriate models remains still an open task. The present paper tackles this problem and points to species interactions as a necessary mechanism to account for them. Specifically, we discuss several possibilities to include interactions in population models and recognize Lotka-Volterra constants as successful ansatz. We design a Bayesian inference algorithm to obtain sets of interaction constants able to reproduce the experimental correlation distributions much better than the state-of-the-art attempts. Importantly, the model still reproduces single-species, experimental, macroecological patterns previously detected in the literature, concerning the abundance fluctuations across both species and communities. Endorsed by the agreement with the observed phenomenology, our analysis provides insights on the properties of microbial interactions, and suggests their sparsity as a necessary feature to balance the emergence of different patterns.

I. INTRODUCTION

Our understanding of the microscopic living world has been recently challenged by the advent of metagenomics [1, 2]. Indeed, DNA sequencing methods unveiled that a large fraction of microbial diversity was missing in laboratory cultures [3–5]. Moreover, the possibility to collect genetic material directly from its natural environment introduced a new dimension—the set of samples—along which the properties of the biome may vary. This has given rise to the production of the largest datasets ever, allowing microbial communities to be investigated at a much greater scale and detail than before.

To approach this new profusion of data, macroecology—the quantitative analysis of emergent broad-scale patterns—prevailed as a promising point of view [6–11]. The framework paved the way to assess statistically the variation in abundance and diversity that, despite the complexity of the underlying microscopic behaviours, often portrays distinctive distributions and that sometimes may be explained in terms of basic ecological forces. Specifically, considerable progress has been achieved in the observation of statistical regularities of taxa populations across time [12], spatial samples [13], and species-abundance distributions [14].

Most remarkably, a recent paper by J. Grilli [15] provided an important step towards a macroecological study of microbial communities. Relying on the analysis of data from nine real biomes, the work characterizes some patterns of abundance variation in terms of three macroecological laws (see Fig.1): *i*) the fluctuations in the abundance of any given species across samples follow a gamma distribution; *ii*) the variances of these distributions for

different species are proportional to the square of their means (Taylor’s law [16]); and *iii*) the mean abundances across species follow a lognormal distribution. These macroecological patterns of species fluctuations and diversity have been parsimoniously explained using the Stochastic Logistic Model (SLM), which endows the traditional logistic equation with a (multiplicative) stochastic term [17, 18] embodying information about environmental variability [15, 19–21].

Beside the aforementioned patterns, the analysis of empirical data unveils also the existence of non-trivial pairwise correlations in species abundances [15]. In particular, the Pearson’s correlation coefficients of all pairs of species in a biome display distributions ranging from anti-correlations to positive correlations, with a peak often located at negative values. These pairwise correlations are not accounted for by the SLM model because it treats species dynamics as independent from each other [22]. Describing correlations in species abundances calls, thus, for introducing some sort of interaction between species.

The existence of species interactions in microbiomes is well documented in a wealth of experimental results that manage to observe and measure them [23–26]. Indeed, microbial interactions are a key ingredient behind community stability [27, 28], necessary for, e.g., the maintenance of health in human biomes [29–31] or the control of medical disorders [32–35]. Though in natural environments species interactions are hard to measure, they can—in principle—be inferred from empirically measured correlations, though this strategy might be plagued with difficulties [36–39]. In any case, there is a broad consensus on the crucial role of interactions in microbial ecosystems, thus pushing for their implementation in current

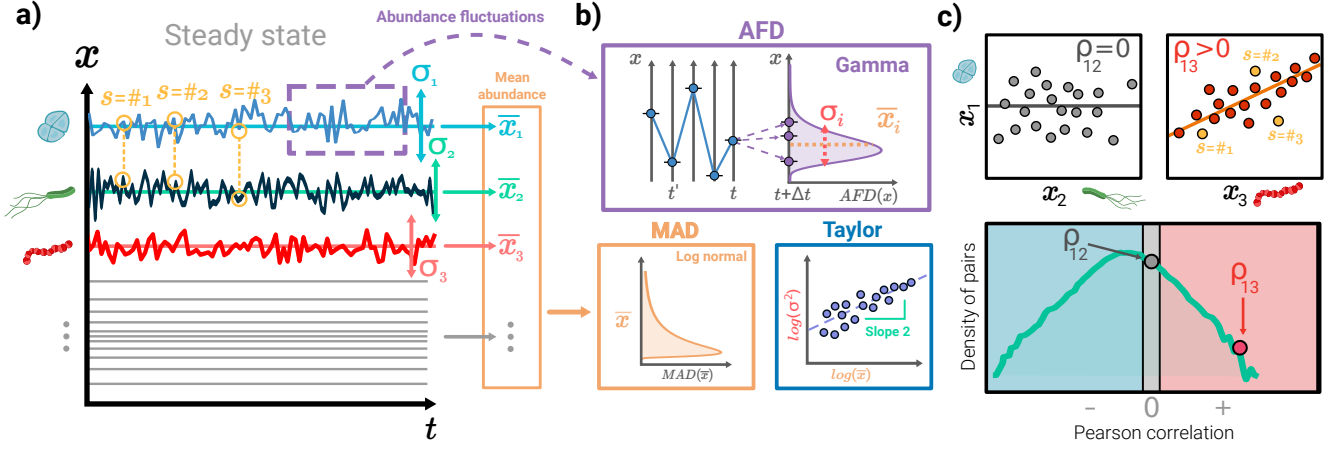


FIG. 1. **Infographic of the population dynamics and the resulting macroecological patterns.** Panel (a) portrays, as an illustrative example, three individual-species (color coded) time courses at equally spaced times (longitudinal data), resulting from the integration of (1). The fluctuations around the mean abundance of each species (abundance fluctuation distribution, AFD) are well described by a gamma distribution, as shown in panel (b) (see Figs. S4 and S5 of the SI). For each species, this distribution is characterized by its mean value \bar{x}_i and its variance σ_i^2 . These two magnitudes are linked by Taylor's law $\sigma_i^2 \propto \bar{x}_i^2$ (panel (b)). The mean abundances of all species are distributed as a lognormal (mean abundance distribution, MAD) (panel (b)). Further details about Taylor's law and MAD are presented in Figs. S6 and S7 of the SI. Panel (c) illustrates the correlations between abundance fluctuations of pairs of species across samples (a point for each sample/realization). The top-left plot illustrates the case of two uncorrelated species whereas the top-right plot illustrates two positively correlated species. The bottom picture shows the distribution of Pearson's coefficients (cf. (3)) of all pairs of species. Empirically, this distribution is found to generally cover the entire range $-1 \leq \rho_{ij} \leq 1$ and to exhibit a peak at negative values.

mechanistic models.

Interactions can be implemented in at least two ways: (i) *indirectly*, i.e. assuming the diverse environmental noise terms to be correlated with each other or (ii) *directly*, i.e. introducing a coupling between species abundances, or (iii) using a combination of both. The first route assumes that correlations in the abundance of two species arise from similar or opposite responses of both species to changes in the environment (variation of nutrients, presence of chemicals, changes in temperature or pH, etc.). This approach has been recently used to reproduce an empirical macroecological pattern describing the decay (on-average) of species pairwise correlations as a function of phylogenetic distance [22]. The second one follows the long tradition in ecology after the seminal works of Lotka and Volterra.

In this paper, we analyze the previous two possibilities as well as their ability to explain empirically observed correlations. For this, we propose a generalized stochastic Lotka-Volterra model (SLVM) involving pairwise deterministic interactions and environmental (multiplicative) fluctuations. Our analyses reveal that direct interactions are most suitable to model the competition mechanisms detected in real biomes and their interplay with cooperative ones, and with other kinds of interdependencies, besides preserving Grilli's three empirical laws. Understanding the mechanisms behind the emergence of these patterns allows us to get an insight into the properties of interaction networks, pointing to their sparsity as a

crucial ingredient.

MODELING MICROBIOMES

Environmental noise vs. species interactions

A simple model that couples species in a parsimonious way is the Stochastic Lotka-Volterra Model (SLVM)

$$\dot{x}_i = \frac{x_i}{\tau_i} \left(1 + \sum_{j=1}^S a_{ij} x_j \right) + x_i \xi_i, \quad i = 1, \dots, S, \quad (1)$$

where τ_i is the time scale of basal population growth, and ξ_i is a zero-mean, multivariate Gaussian white noise (Itô interpretation) with correlations $\langle \xi_i(t) \xi_j(t') \rangle = w_{ij} \delta(t - t')$. The matrix $\mathbf{W} = (w_{ij})$ accounts for environmental fluctuations, whereas the off-diagonal terms of matrix $\mathbf{A} = (a_{ij})$ describe direct, Lotka-Volterra-like interactions between species, and the diagonal terms $a_{ii} = -1/K_i$ incorporate the carrying capacity of the environment for species i .

When $\mathbf{W} = w\mathbf{I}$ and \mathbf{A} is a diagonal matrix, (1) becomes the SLM. By turning on the off-diagonal terms of the noise correlation matrix \mathbf{W} ("indirect interactions") and/or of the Lotka-Volterra matrix \mathbf{A} ("direct interactions"), we can study the effect of correlated environmental noise and/or direct species interactions on species

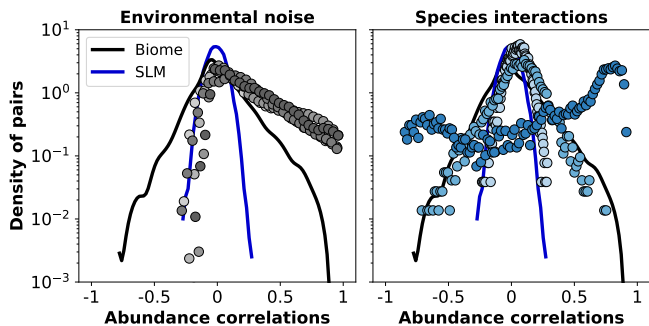


FIG. 2. Distributions of Pearson’s abundance correlation coefficients (c.f. (3)) as obtained in the model with (left panel) a few samples of the noise correlation matrix \mathbf{W} (each with a different gray shade) or (right panel) with random samples of the Lotka-Volterra matrix \mathbf{A} . The black solid lines portray in each case the empirical distribution as obtained from the *Sea-water* microbiome (species which appear in less than 50% of the communities have been filtered out), while the blue ones represent the distribution of correlations as obtained from the model without interactions. In the left plot, colored circles show the results for a few samples of matrices \mathbf{W} (see ‘Material and methods’ for details of the sampling procedure); Lotka-Volterra constants are chosen as $a_{ij} = -\delta_{ij}/K_i$, with carrying capacities K_i sampled from a lognormal distribution with mean 0.1 and standard deviation 0.5—as for the SLM [15]. The results shown in this figure are typical (the SI shows the results for a larger sample). In the right plot, colored circles represent correlations resulting from the SLVM with $\mathbf{W} = w\mathbf{I}$ and Lotka-Volterra constants a_{ij} ($i \neq j$) sampled from a Gaussian distribution with zero mean and standard deviation 0.03. A random selection of 60% of such constants are set to zero (i.e. the connectance of the interaction matrix is $C = 0.4$).

pairwise correlations. Ideally, though, the model should contain the “right proportion” of both terms.

At first, sight, adding environmental noise (\mathbf{W}) has an advantage over adding interactions (\mathbf{A}) in that Grilli’s first law is preserved by construction (see Sec. 8A of the Supporting Information). The second law simply amounts to setting $w_{ii} = w$ for all i . As for the third law, it can be fulfilled if one chooses ad hoc the carrying capacities K_i as lognormal random variables [15]. Obviously, these latter choices do not explain the origin of the second and third laws, but at least render a model that is compatible with them. On the downside though, the fact that \mathbf{W} , by definition, must be symmetric and positive definite severely constrains the kind of abundance correlations that (1) can generate.

If we introduce interactions while keeping $\mathbf{W} = w\mathbf{I}$, in general the first and second laws do not hold exactly—although they may approximately do so. However, the presence of interactions strongly affects the average abundance of the species. While the SLM (with or without a noise correlation matrix) predicts a stationary population that fluctuates around its carrying capacity, in the presence of coupling, the mean values are the solution of

the linear system (see Sec. 2 of the SI)

$$\sum_{j=1}^S a_{ij} \bar{x}_j = \frac{\tau_i w}{2} - 1, \quad i = 1, \dots, S, \quad (2)$$

where \bar{x}_j denotes the average abundance of species j . Therefore interactions shift these average abundances to the extent that, even if all carrying capacities were the same, the \bar{x}_j would split over a range of values. This may not be a full explanation of the third law yet, but it opens the possibility that its origin might lie on a particular structure of the network of interactions.

A quick test to decide which of these two approaches is most promising to model abundance correlations is to generate a large sample of random matrices (either \mathbf{W} or \mathbf{A}), and for each of them simulate the stochastic process (1), calculate abundance correlations between pairs of species, and compare the resulting distributions with those empirically obtained from the microbiome datasets with the same number of species (Fig. 1a and c). Each of these two samples must fulfill some constraints: matrices \mathbf{W} must all be symmetric and positive definite, and matrices \mathbf{A} must all lead to a *feasible* (i.e. $\bar{x}_i > 0$ for all i) [40] and *asymptotically stable* (i.e. small perturbations must die out [41, 42]) steady state (see Secs. 3 and 4 of the SI).

Figure 2 shows the distribution of Pearson’s abundance correlation coefficients

$$\rho_{ij} = \frac{\text{Cov}(x_i, x_j)}{\sqrt{\text{Var}(x_i) \text{Var}(x_j)}}, \quad (3)$$

for all $S(S-1)$ pairs of species $i \neq j$, as obtained from a typical dataset and using each of these two matrix ensembles. The empirical distribution decays exponentially to the left and to the right, is a bit asymmetrical, and has a peak at slightly negative values of the correlation. The distributions obtained from the \mathbf{W} samples bear little resemblance to the former—they exhibit very little negative correlations, are strongly asymmetric, and show a peak at zero. On the contrary, distributions obtained from the \mathbf{A} samples have a wide range of sample to sample variability, and some of the realizations are very similar to empirical data, often peaking at negative correlation values.

These analyses suggest that environmental noise by itself seems incapable of generating correlations resembling those observed in real microbiomes, and so interactions have to be included in the model. In any case, the presence of correlated noise cannot be ruled out from these analyses, but in order to keep things simple, we henceforth take $\mathbf{W} = w\mathbf{I}$ and focus on the effect of interactions in the model.

Grilli’s laws in the presence of interactions

The model described by (1) with $\mathbf{W} = w\mathbf{I}$ and a non-trivial interaction matrix \mathbf{A} is not guaranteed to satisfy

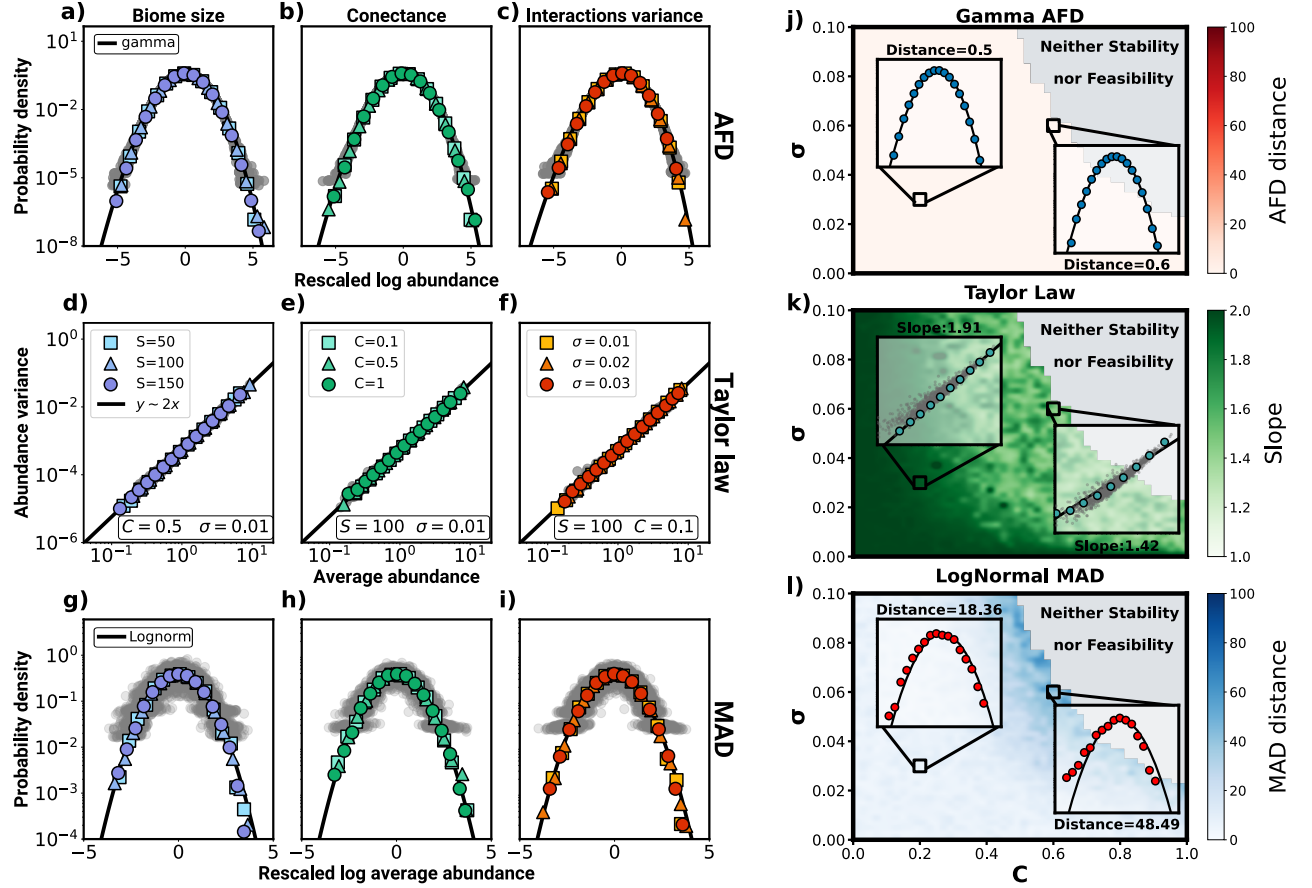


FIG. 3. Grilli's three macroecological laws as a function of the interaction parameters. Specifically, the figure shows the abundance fluctuation distribution (AFD) (panels (a)–(c)), Taylor's law (panels (d)–(f)) and the mean-abundance distribution (MAD, panels (g)–(i)) for different values of the species number S (panels (a), (d), (g)), the connectance C (panels (b), (e), (h)), and standard deviation of the interaction constants σ (panels (c), (f), (i)). Results have been averaged over $N = 1000$ realizations of the SLVM ((1)) each one with a different random interaction matrix. Results including all realizations are depicted as a cloud of gray points, whereas averages are shown as colored bullets. The AFD obtained for a given realization contains the results for all species, represented in terms of rescaled logarithm abundances ($z = \text{Var}(x)^{-1/2} \log(x/\bar{x})$). Solid black lines correspond to gamma distributions. MAD plots (g)–(i) is obtained by properly rescaling the mean abundances, and are fitted by a normalized (zero mean, unit standard deviation) lognormal distribution (black solid line). Similarly, the black straight lines in panels (d)–(f) describe the relation $\text{Var}(x_i) \propto \bar{x}_i^2$ in logarithmic scale. All simulations are performed with $S = 50$, $\tau_i = 0.1$, $w = 0.1$, and carrying capacities sampled from a lognormal distribution (mean 0.1, standard deviation 0.5). Panels: (j), (k), (l) illustrate the limits of the weak-interaction regime across the set of parameters that characterize species interactions. The plots quantify the compliance with (j) a gamma AFD, (k) Taylor's law, and (l) a lognormal MAD, within the region where the system is stable and feasible. Each pixel corresponds to a combination of values of the network connectance C (horizontal axis) and the standard deviation σ of the distribution of interactions (vertical axis). The color of the pixel quantifies the distance from the AFD to a gamma distribution (j), the value of the exponent γ in the relationship $\text{Var}(x_i) \propto \bar{x}_i^\gamma$ (k), and the distance of the MAD to a lognormal distribution (l), averaged over a sample of $N = 100$ realizations. Gray areas mark the region of the parameter space where the resulting systems are neither stable nor feasible.

any of the three macroecological laws found by Grilli [15]—even if the carrying capacities K_i are sampled from a lognormal distribution, as in the SLM. However, as long as the interactions are a ‘small’ perturbation to the SLM, one can reasonably expect them to hold, at least approximately. In particular, if one sets a fraction C (‘connectance’) of the off-diagonal interactions terms to zero, and chooses the rest randomly and independently from

a zero-mean normal distribution with standard deviation σ , a criterion for the weakness of interactions is that the resulting system remains feasible and asymptotic stable; in other words, $\sigma\sqrt{SC}K_{\max} \ll 1$ (see Sec. 5 of the SI). We will refer to this as the ‘weak-interaction regime’.

Figure 3 shows the compliance with the three macroecological laws for different combinations of parameters within the weak-interaction regime (see Fig. 1a and b for

the sampling procedure). The first row illustrates that fluctuations of the abundance around the mean values still follow a gamma distribution (first law); the second row reveals that $\text{Var}(x_i) \propto \bar{x}_i^2$, according to Taylor’s law (second law); and the third row shows that the mean abundances very closely follow a lognormal distribution (third law). Particularly noteworthy is the compliance with the third law, given that the mean abundances are no longer fixed by the carrying capacities (see (2)), which do follow a lognormal distribution.

Importantly, the gamma abundance-fluctuation distribution remains unaffected regardless of the values taken by the interaction parameters (Fig. 3j). Moving closer to the boundary of the weak-interaction regime we can see Taylor’s law still holds, but the exponent gets modified as $\text{Var}(x_i) \propto \bar{x}_i^\gamma$. As this boundary is approached, the exponent decreases down to values around $\gamma \approx 1.4$ (Fig. 3k) and, likewise, the distance between the distribution of mean abundances and a lognormal increases (Fig. 3l), although it is never very large.

It is worth mentioning that the SLVM ((1)) provides an alternative way to comply with the third law other than sampling the carrying capacities from a lognormal distribution and remaining in the weak-interaction regime. Even if we choose constant carrying capacities ($K_i = K$ for all i), (2) allows us to seek interaction matrices that shift the mean abundances so as to follow a lognormal distribution. In Section 6 of the SI shows that such matrices do actually exist and yield stable and feasible communities. This finding brings species interactions in the long debate about the origin of heavy-tailed abundance distributions, something which, to the best of our knowledge, has been scarcely investigated. This is an issue that goes beyond the aim of the current work and will be explored in a forthcoming publication. Therefore, hereafter we focus on the weak-interaction regime with log-normally distributed carrying capacities.

Interactions reproduce the distribution of correlations

An analysis of empirical data selected from the *EBI metagenomics* platform [43] reveals that, on top of the three single-species, macroecological laws that we have discussed so far, microbiomes exhibit pairwise correlations. As a matter of fact, the distribution of all $S(S-1)$ Pearson’s coefficients (c.f. (3)) of a microbial community has a characteristic pattern (Fig. 1c). For all the microbiomes that we have considered, this distribution approximately covers the whole range of values ($-1 \leq \rho_{ij} \leq 1$), and is very different from the residual narrow distribution peaked at zero that results from the approach with no species interactions [15, 19, 20] (see Fig. 2, as well as Fig. 4a). Worth noticing is the almost exponential decay to both sides of the interval, and the location of the maximum at neatly negative values of ρ_{ij} .

In order to find a set of interaction matrices \mathbf{A} which

are capable of inducing this type of correlations, while at the same time preserving Grilli’s three laws, we have adopted a Bayesian approach. We know from the previous analysis (Fig. 2 right) that matrices inducing correlations distributed similarly to the empirical ones do exist. Thus, we take the empirical distributions as given—within a Gaussian error—and wonder about the posterior probability distribution of interaction matrices \mathbf{A} . Needless to say, this distribution cannot be computed analytically, so in order to sample matrices \mathbf{A} out of the ensemble of possible solutions we need to perform a Markov-chain Monte Carlo (MCMC) simulation (see ‘Materials and methods’ for the details).

As an illustration of the results of this approach, Fig. 4a shows the distribution of Pearson’s coefficients obtained for five biomes (See Fig. S17 of the SI contains the results for all available biomes in our dataset), along with the empirical ones. The figure is very eloquent as it reveals a very precise agreement in all cases. Remarkably, these results are obtained when the interaction matrix \mathbf{A} is still very sparse, as Fig. 4b illustrates—a value for which the three macroecological laws hold in the presence of interactions (see Fig. 3). As a consistency test, we have checked that this is indeed the case for the particular matrices \mathbf{A} obtained through the MCMC (See Figs. S18, S19, S20 of the SI).

It is worth mentioning that similar results to those of Fig. 4a can be obtained for matrices with a higher connectance (see bottom plot of Fig. 4b). However, these matrices usually produce a lower exponent in Taylor’s (second) law, as well as a distribution of mean abundances that deviates from a lognormal distribution (third law). We have performed a different MCMC in which the empirical mean-abundance distribution is taken as given, and indeed we then can fix the first and third law, but not the exponent of the second. While we cannot rule out the possibility that highly connected matrices can achieve similar accuracy in reproducing the correlations without spoiling the macroecological laws, our results strongly suggest that a low connectance of the network of interactions might be an important feature of real microbiomes. This seems to be consistent with existing experimental evidence [23, 26].

DISCUSSION

The recent discovery of universal large-scale patterns in natural bacterial communities opens the way to empirically validate possible ecological models [15]. While the properties of species-abundance fluctuations constrain the models to include stochastic environmental fluctuations, the pattern of pairwise correlations can reveal the nature and structure of species interactions. This is a promising direction because it is well documented that species interactions play a fundamental role in the behaviour of microbial communities. As a matter of fact, they may underlie the critical features associated, e.g.,

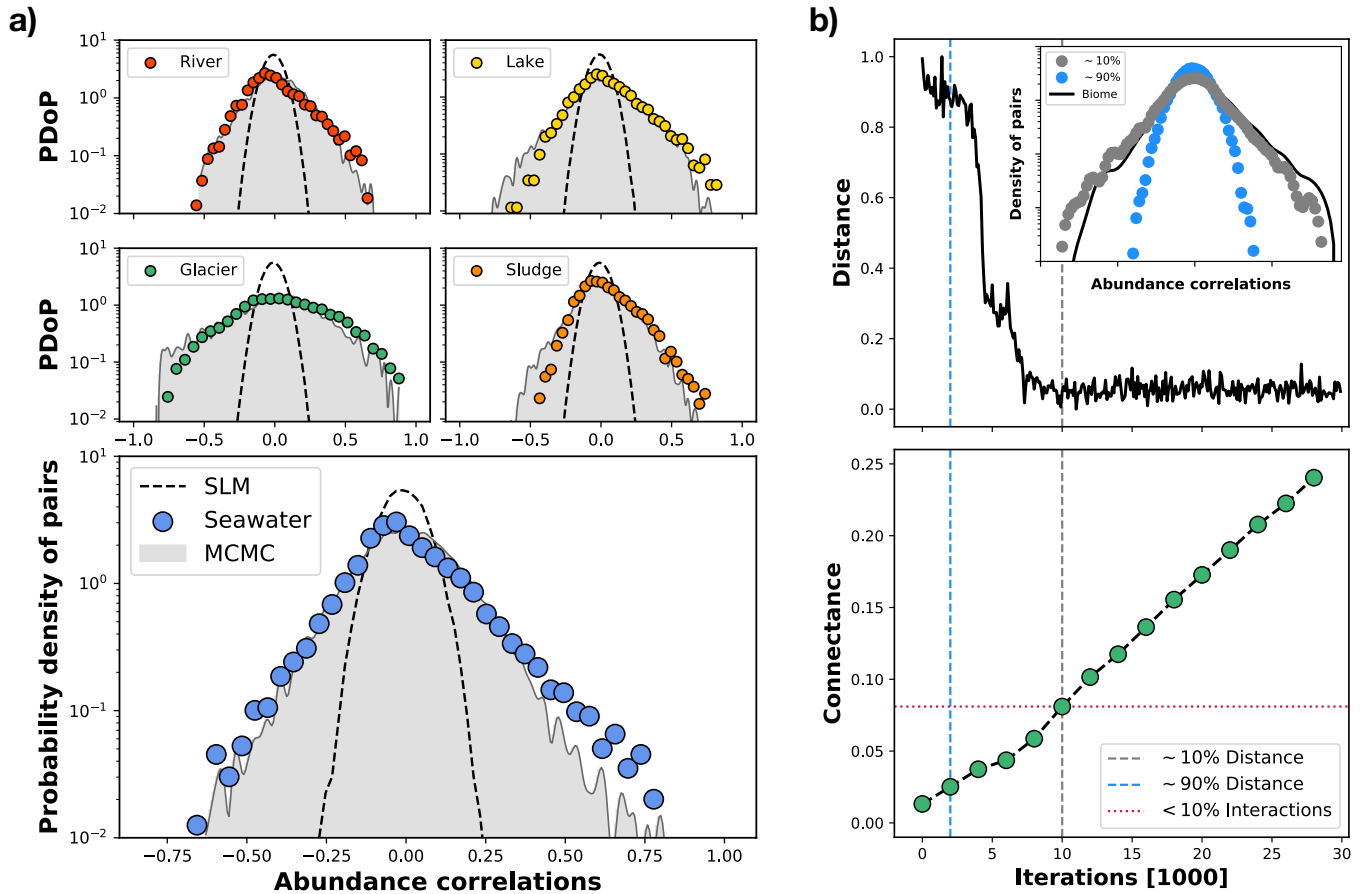


FIG. 4. Abundance correlation distributions for real and simulated communities. In (a), different colored bullets correspond to different biomes selected from the *EBI metagenomics* platform [43] (namely Seawater, River, Lake, Glacier and Sludge communities). Black dashed lines portray the distribution of Pearson’s coefficients for the abundance correlation of all pairs of species resulting from the SLM. Gray curves show the same distributions as obtained from the SLVM (c.f. (1)), with the Lotka-Volterra interaction constants inferred using the Bayesian algorithm described in Material and methods. The top panel of (b) shows the Euclidean distance between the log-distributions of Pearson’s correlation coefficients of pairs of species, as obtained from simulations and from empirical data (*Seawater* using only species appearing in at least 50% of the samples), as a function of the iterations of the MCMC. The bottom panel shows the connectance C of the inferred interaction matrices as a function of iterations. The inset illustrates the distributions after 2000 iterations—where the distance is still large—and after 10000 iterations—where the distance has dropped below 10% of the initial distance. Remarkably, this iteration corresponds to a network with a connectance $C \approx 0.1$, suggesting that a small fraction of interactions is enough to reproduce the distribution of correlations. See Figs. S21 and S22 of the SI for similar results in the rest of the considered biomes.

with health disorders [32], such as Crohn’s disease [33] or other forms of inflammatory bowel syndrome [34], and many current treatments rely on competition among bacteria [31, 35].

However, neither the SLM nor any other single-species approach is able to account for the abundance correlation patterns that these communities exhibit. It is true that the existence of a correlation between a pair of species does not necessarily imply a direct interaction between them—it may be caused by similar or opposite responses to environmental fluctuations or external driving forces. As a matter of fact, a recent work has shown that environmental filtering, i.e. the presence of correlated external noise, is the main driver of pairwise species correlations

at small phylogenetic distances (i.e. with specific taxa) [22]. Nevertheless, species correlations emerge also between diverse taxa and hence, other ecological interactions must also be at play. Furthermore, the widespread presence of negative correlations renders this explanation incomplete.

In this paper, we have shown that a generalized Lotka-Volterra model comprising species pairwise interactions and stochastic environmental fluctuations can reproduce the empirical distribution of species correlations. This conclusion is also supported by a recent work where microbial communities are investigated within the framework of a consumer-resource model, with the conclusion that competition for resources can account for diverse

statistical patterns across diverse microbiomes. [44].

Furthermore, we have shown that the model including species interactions complies with the three Grilli’s macroecological laws as well as with the empirical pattern of abundance pairwise correlation, simultaneously. In particular, we have found that sparse interaction matrices are able to achieve all these goals, in agreement with the empirically reported sparsity of microbial interaction networks [23, 26]. More specifically, we have observed that the set of interaction matrices leading to correlations compatible with the empirical ones nearly overlaps with the set of matrices rendering the model feasible and asymptotically stable, provided one accepts that the exponent of Taylor’s law can be less than 2. Whether this is a weakness of the model or a prediction that some communities may exhibit this extended version of Taylor’s law remains to be explored.

We are aware that some modelling choices can be questioned. For instance, the use of pairwise interactions in a Lotka-Volterra-like fashion. Apart from its long tradition in theoretical ecology, recent works [45, 46] show that, within some limits, it is a reasonable choice. Nevertheless, it has been argued that higher-order interactions may be crucial in the correct assessment of community stability and the understanding of its conflicting relationship with species diversity [40, 47]. Microbiomes are extraordinarily complex communities where processes involving more than two species may be prevalent [48]. Therefore, including higher-order interaction terms in (1) is a generalization worth exploring.

Aside from these obvious limitations, our analysis offers many possibilities to reach a deeper understanding of microbial communities and their emerging ecological patterns. For instance, whereas the origin of the gamma abundance fluctuations distribution—and its cousin, Taylor’s law—is related to the multiplicative nature of the noise (the larger the abundance the larger its fluctuations), we still lack a good explanation for the appearance of a lognormal mean-abundance distribution. Both, in the SLM and the present SLVM it has been imposed by purposely tailoring the carrying capacities of the species. But through (2), the SLVM offers the possibility that a special choice of the interaction constants—away from what we have termed weak-interaction regime—may induce a lognormal mean abundance distribution in some self-organized way. Preliminary analyses show that this can indeed happen (see Sec. 6 of the SI), placing the explanatory burden on the nature of the interaction networks. This launches network theory of species interactions in the long-lasting debate [49] about the origin of mechanistic processes behind the emergence of heavy-tailed species-abundance distributions—something that, to the best of our knowledge has been scarcely explored so far (see [50] for an exception). More generally, our work indicates that empirical correlations and fluctuation patterns can be reproduced by a large diversity of possible interaction matrices. In future works we will characterize such a matrix

ensemble, with the ambitious goal of extrapolating its minimal structural features allowing one to understand and simulate in-silico complex microbial communities.

Perhaps the most important message of the present work is that direct interactions between species are as relevant in microbiomes as they are in other more traditional ecosystems—such as animal-plant communities or food webs. In this regard, our analysis brings the study of microbes closer to the well-established framework of community ecology, where generalized Lotka-Volterra models play a central role. This paves the way to testing theoretical laws in ecology through experiments performed in microbial communities. The test of the stability-diversity relationship carried out in Ref. [51] is an excellent example of this idea. In view of the usual scarcity of data for traditional ecosystems, the overwhelming amount of microbial data provided by metagenomics opens an avenue of unprecedented possibilities for ecology.

MATERIAL AND METHODS

Numerical solution of the SLVM

Equation (1) was solved numerically using an Euler-Maruyama integration scheme [52]. For each species, the solution depicts a noisy logistic trajectory, with the stationary mean population set by the interaction properties. In this framework, the population of a given species in different samples may be recovered, once the dynamics have reached the stationary state, by either selecting abundances at different times (longitudinal data) or considering the abundances of different realizations at the same time (cross-sectional data). Both ways lead to identical results (i.e., the system is ergodic). Further details are discussed in Sec. 1 of the SI.

Environmental noise matrix sampling

To produce a random, positive definite, symmetric matrix \mathbf{W} we factor it as $\mathbf{W} = \mathbf{U}\mathbf{\Lambda}\mathbf{U}^t$, where \mathbf{U} is an $S \times S$ orthogonal matrix ($\mathbf{U}\mathbf{U}^t = \mathbf{U}^t\mathbf{U} = \mathbf{I}$) and $\mathbf{\Lambda}$ is a diagonal matrix whose diagonal elements are random, non-negative real numbers (see S5 of the SI for a full account.). The orthogonal matrix \mathbf{U} can be generated by randomly sampling from a Haar distribution (generated using the Python function `ortho_group` from the SciPy package [53]).

Bayesian approach

The posterior distribution of matrix \mathbf{A} , given the correlation distribution ρ , is obtained as

$$P(\mathbf{A}|\rho) = \frac{P(\rho|\mathbf{A})P(\mathbf{A})}{P(\rho)}. \quad (4)$$

In order to sample matrices \mathbf{A} from the posterior distribution $P(\mathbf{A}|\rho)$ we apply a Metropolis-Hastings factor algorithm [52]. This amounts to replacing those samples by samples of a purposely tailored Markov chain. At each step n of this chain, a pair of species (i, j) is randomly selected and its corresponding interaction constant gets modified as $a_{ij}^{(n+1)} = a_{ij}^{(n)} + \eta$, where η is a random variable sampled from an uniform distribution in $(-\epsilon, \epsilon)$. This change is accepted with probability $\min(1, H_n)$ —otherwise rejected—where the Hasting factor (using Bayes’s formula (4)) is obtained as

$$H_n = \frac{P(\rho|\mathbf{A}^{(n+1)})P(\mathbf{A}^{(n+1)})}{P(\rho|\mathbf{A}^{(n)})P(\mathbf{A}^{(n)})}.$$

The likelihood is computed as

$$P(\rho|\mathbf{A}) \propto \exp \left\{ -\frac{1}{2\Delta^2} \sum_i \log^2 \left(\frac{\rho(x_i)}{\hat{\rho}(x_i)} \right) \right\},$$

where $\rho(x)$ is the empirical distribution of Pearson’s coefficients, $\hat{\rho}(x)$ is the one computed using matrix \mathbf{A} , and Δ is the error in the empirical data (experiments have been performed by considering different values for this quantity in the range $0.2 \leq \Delta \leq 1$, with similar results). As for the prior $P(\mathbf{A})$, we choose it to be zero if \mathbf{A} leads to an unstable or unfeasible community, and constant otherwise. Finally, ϵ is selected so as to keep an acceptance ratio along the Markov chain of $\sim 30\%$.

ACKNOWLEDGMENTS

This work has been supported by (i) grants PGC2018-098186-B-I00 (BASIC), PID2021-128966NB-I00, and PID2020-113681GB-I00 of the Spanish Ministry and Agencia Estatal de Investigación (MCIN/AEI/10.13039/501100011033), and by the European Regional Development Funds (ERDF) “A way of making Europe”; and (ii) project B-FQM-366-UGR20 (ERDF) of the Consejería de Conocimiento, Investigación y Universidad, Junta de Andalucía and Universidad de Granada. We also thank Jacopo Grilli for a critical reading of the manuscript.

-
- [1] J. Handelsman, M. R. Rondon, S. F. Brady, J. Clardy, and R. M. Goodman, *Chemistry and Biology* **5**, R245 (1998).
 - [2] H. L. Steele and W. R. Streit, *FEMS Microbiology Letters* **247**, 105 (2005), <https://academic.oup.com/femsle/article-pdf/247/2/105/19122132/247-2-105.pdf>.
 - [3] W. B. Whitman, D. C. Coleman, and W. J. Wiebe, *Proceedings of the National Academy of Sciences* **95**, 6578 (1998), <https://www.pnas.org/doi/pdf/10.1073/pnas.95.12.6578>.
 - [4] M. S. Rappé and S. J. Giovannoni, *Annual Review of Microbiology* **57**, 369 (2003), pMID: 14527284, <https://doi.org/10.1146/annurev.micro.57.030502.090759>.
 - [5] L. A. Hug, B. J. Baker, K. Anantharaman, C. T. Brown, A. J. Probst, C. J. Castelle, C. N. Butterfield, A. W. Hersndorf, Y. Amano, K. Ise, Y. Suzuki, N. K. Dudek, D. A. Relman, K. Finstad, R. Amundson, B. C. Thomas, and J. F. Banfield, *Nature Microbiology* **1**, 16048 (2016).
 - [6] J. H. Brown and B. A. Maurer, *Science* **243**, 1145 (1989).
 - [7] J. H. Brown, *Macroecology* (University of Chicago Press, 1995).
 - [8] R. Field, *Global Ecology and Biogeography* **11**, 87 (2002).
 - [9] J. I. Prosser, B. J. Bohannan, T. P. Curtis, R. J. Ellis, M. K. Firestone, R. P. Freckleton, J. L. Green, L. E. Green, K. Killham, J. J. Lennon, *et al.*, *Nature Reviews Microbiology* **5**, 384 (2007).
 - [10] A. Shade, R. R. Dunn, S. A. Blowes, P. Keil, B. J. Bohannan, M. Herrmann, K. Küsel, J. T. Lennon, N. J. Sanders, D. Storch, and J. Chase, *Trends in Ecology & Evolution* **33**, 731 (2018).
 - [11] B. J. McGill, *Global Ecology and Biogeography* **28**, 6 (2019), <https://onlinelibrary.wiley.com/doi/pdf/10.1111/geb.12855>.
 - [12] B. W. Ji, R. U. Sheth, P. D. Dixit, K. Tchourine, and D. Vitkup, *Nature Microbiol.* **5**, 768 (2020).
 - [13] S. Zaoli and J. Grilli, *Science Adv.* **7**, eabj2882 (2021).
 - [14] W. R. Shoemaker, K. J. Locey, and J. T. Lennon, *Nature Ecol. Evol.* **5**, 1 (2017).
 - [15] J. Grilli, *Nature Comm.* **11**, 1 (2020).
 - [16] L. R. Taylor, *Nature* **189**, 732 (1961).
 - [17] S. Redner, *American Journal of Physics* **58**, 267 (1990).
 - [18] M. A. Muñoz, F. Colaiori, and C. Castellano, *Physical Review E* **72**, 056102 (2005).
 - [19] L. Descheemaeker and S. de Buyt, *eLife* **9**, e55650 (2020).
 - [20] R. Wolff, W. Shoemaker, and N. Garud, *mBio* **14**, e02502 (2023), <https://journals.asm.org/doi/pdf/10.1128/mbio.02502-22>.
 - [21] W. R. Shoemaker, *bioRxiv* **10.1101/2022.04.07.487434** (2023), <https://www.biorxiv.org/content/early/2023/05/25/2022.04.07.487434>.
 - [22] M. Sireci, M. A. Muñoz, and J. Grilli, *bioRxiv* **10.1101/2022.07.12.499693** (2023), <https://www.biorxiv.org/content/early/2023/02/10/2022.07.12.499693>.
 - [23] J. Kehe, A. Ortiz, A. Kulesa, J. Gore, P. C. Blainey, and J. Friedman, *Science Advances* **7**, eabi7159 (2021), <https://www.science.org/doi/pdf/10.1126/sciadv.abi7159>.
 - [24] J. Hu, D. R. Amor, M. Barbier, G. Bunin, and J. Gore, *Science* **378**, 85 (2022), <https://www.science.org/doi/pdf/10.1126/science.abm7841>.
 - [25] S. A. Shetty, B. Kuipers, S. Atashgahi, S. Aalvink, H. Smidt, and W. M. de Vos, *Biofilms and Microbiomes* **8**, 21 (2022).

- [26] A. S. Weiss, A. G. Burrichter, A. C. Durai Raj, A. von Stempel, C. Meng, K. Kleigrew, P. C. Münch, L. Rössler, C. Huber, W. Eisenreich, L. M. Jochum, S. Göing, K. Jung, C. Lincetto, J. Hübner, G. Marinos, J. Zimmermann, C. Kaleta, A. Sanchez, and B. Stecher, *The ISME Journal* **16**, 1095 (2022).
- [27] C. KZ, S. J, and F. KR, *Science* **350**, 663 (2015).
- [28] S. Butler and J. P. O'Dwyer, *Nature Comm.* **9**, 2970 (2018).
- [29] C. A. Lozupone, J. I. Stombaugh, J. I. Gordon, J. K. Jansson, and R. Knight, *Nature* **489**, 220 (2012).
- [30] D. A. Relman, *Nutr. Rev.* **70**, S2 (2012).
- [31] J. de Dios Caballero, R. Vida, M. Cobo, L. Máiz, L. Suárez, J. Galeano, F. Baquero, R. Cantón, and R. del Campo, *mBio* **8**, e00959 (2017).
- [32] P. D. Newell and A. E. Douglas, *Appl. Env. Microbiol.* **80**, 788 (2014).
- [33] S. Khanna and L. E. Raffals, *Gastroenterol. Clin. N. Am.* **46**, 481 (2017), crohn's Disease.
- [34] D. N. Frank, A. L. S. Amand, R. A. Feldman, E. C. Boedeker, N. Harpaz, and N. R. Pace, *Proc. Natl. Acad. Sci. USA* **104**, 13780 (2007).
- [35] J. D. Palmer and K. R. Foster, *Science* **376**, 581 (2022).
- [36] Y. Xiao, M. T. Angulo, J. Friedman, M. K. Waldor, S. T. Weiss, and Y.-Y. Liu, *Nature Comm.* **8**, 2042 (2017).
- [37] M. T. Angulo, C. H. Moog, and Y.-Y. Liu, *Nature Comm.* **10**, 1045 (2019).
- [38] M. S. Matchado, M. Lauber, S. Reitmeier, T. Kacprowski, J. Baumbach, D. Haller, and M. List, *Comput. Struc. Biotech. J.* **19**, 2687 (2021).
- [39] S. Pinto, E. Benincà, E. H. van Nes, M. Scheffer, and J. A. Bogaards, *PLoS Comp. Biol.* **18**, e1010491 (2022).
- [40] J. Grilli, G. Barabás, M. J. Michalska-Smith, and S. Allesina, *Nature* **548**, 210 (2017).
- [41] R. May, *Nature* **238**, 413 (1972).
- [42] S. Allesina and S. Tang, *Nature* **483**, 205 (2012).
- [43] A. L. Mitchell, M. Scheremetjew, H. Denise, S. Potter, A. Tarkowska, M. Qureshi, G. A. Salazar, S. Pesseat, M. A. Boland, F. M. I. Hunter, P. Ten Hoopen, B. Alako, C. Amid, D. J. Wilkinson, T. P. Curtis, G. Cochrane, and R. D. Finn, *Nucleic Acids Res.* doi: 10.1093/nar/gkx967 (2018).
- [44] P.-Y. Ho, B. H. Good, and K. C. Huang, *eLife* **11**, e75168 (2022).
- [45] Tyler A. Joseph and Liat Shenhav and Joao B. Xavier and Eran Halperin and Itsik Pe'er, *PLoS Comput. Biol.* **16**, e1007917 (2020).
- [46] S. Dedrick, V. Warriar, K. P. Lemon, and B. Momeni, *bioRxiv* 10.1101/2022.08.08.503228 (2022).
- [47] E. Bairey, E. D. Kelsic, and R. Kishony, *Nature Communications* **7**, 12285 (2016).
- [48] W. B. Ludington, *Trends in Microbiology* **30**, 618 (2022).
- [49] B. J. McGill, R. S. Etienne, J. S. Gray, D. Alonso, M. J. Anderson, H. K. Benecha, M. Dornelas, B. J. Enquist, J. L. Green, F. He, A. H. Hurlbert, A. E. Magurran, P. A. Marquet, B. A. Maurer, A. Ostling, C. U. Soykan, K. I. Ugland, and E. P. White, *Ecol. Lett.* **10**, 995 (2007).
- [50] W. G. Wilson, P. Lundberg, D. P. Vázquez, J. B. Shurin, M. D. Smith, W. Langford, K. L. Gross, and G. G. Mittelbach, *Ecology Letters* **6**, 944 (2003), <https://onlinelibrary.wiley.com/doi/pdf/10.1046/j.1461-0248.2003.00521.x>.
- [51] Y. Yonatan, G. Amit, J. Friedman, and A. Bashan, *Nature Ecol. Evol.* **6**, 693 (2022).
- [52] R. Toral and P. Colet, *Stochastic Numerical Methods* (Wiley-VCH, Weinheim, Germany, 2014).
- [53] P. Virtanen, R. Gommers, T. E. Oliphant, M. Haberland, T. Reddy, D. Cournapeau, E. Burovski, P. Peterson, W. Weckesser, J. Bright, S. J. van der Walt, M. Brett, J. Wilson, K. J. Millman, N. Mayorov, A. R. J. Nelson, E. Jones, R. Kern, E. Larson, C. J. Carey, Í. Polat, Y. Feng, E. W. Moore, J. VanderPlas, D. Laxalde, J. Perktold, R. Cimrman, I. Henriksen, E. A. Quintero, C. R. Harris, A. M. Archibald, A. H. Ribeiro, F. Pedregosa, P. van Mulbregt, and SciPy 1.0 Contributors, *Nature Methods* **17**, 261 (2020).